V European Conference on Computational Fluid Dynamics
ECCOMAS CFD 2010
J. C. F. Pereira and A. Sequeira (Eds)
Lisbon, Portugal,14-17 June 2010

MIMETIC SPECTRAL ELEMENT METHOD FOR GENERALIZED CONVECTION-DIFFUSION PROBLEMS

J.J. Kreeft*, A. Palha† and M.I. Gerritsma†

*Delft University of Technology, Faculty of Aerospace Engineering,
Kluyverweg 2, 2629 HT Delft, The Netherlands
e-mail: J.J.Kreeft@tudelft.nl
†Delft University of Technology, Faculty of Aerospace Engineering,
Kluyverweg 2, 2629 HT Delft, The Netherlands
e-mail: {A.Palha,M.I.Gerritsma}@tudelft.nl

Key words: Mimetic discretization, differential geometry, Spectral Element Method, convection-diffusion

Abstract. *In the last few decades geometrically-derived techniques to discretize partial differential equation encounter increasing popularity, because of their structure-preserving properties. These techniques make use of differential geometry to formulate the partial differential equations in continuous space and use algebraic topology as its discrete counterpart. In algebraic topology variables can be prescribed on different kinds of geometric objects, like points, lines, surfaces, volumes, but also space-time objects.*

Moreover differential geometry and algebraic topology lead to a representation that clearly separates the pure topological and the metric dependent part of the PDE and its discretization. Methods based on these principles are known as mimetic techniques, since they mimic the underlying geometric structures.

The mimetic spectral element method presented is based on Lagrange and edge interpolants that satisfy the mimetic properties and are able to reconstruct differential forms from cochains.

The discretization is explained using a number of sample problems and some numerical examples are given to demonstrate the possibilities of the method presented.

1 INTRODUCTION

In continuum mechanics, physics is mathematically expressed in terms of partial differential equations. These PDE's often can be split up in a set of first-order differential equations representing conservation and equilibrium laws and a set of constitutive relations, where the former laws are pure topological relations between physical quantities and the latter contains all the metric dependence. Unfortunately, solutions of these PDE's are in general not known and therefore numerical methods are required. This work focuses on mimetic discretization techniques. Mimetic discretizations aim to preserve as many symmetries of the PDE's as possible, by mimicking the properties of the PDE's in the discretization[3–5,12,15]. For example think of the gradient, Stokes' and Gauss' theorems that can be applied to the set of first-order differential equations. These theorems relate operator like grad, curl and div that act on physical quantities in the PDE's to the geometric objects on which these physical quantities are defined. These theorems show that different physical quantities in general live on different geometric objects. When physical quantities are expressed using scalars and vectors the connection with their geometric objects is unclear. A mathematical tool that is able to relate quantities with their type of geometric objects is the *differential form*. Differential forms can be seen as the things which occur under an integal. Differential forms are described by *differential geometry*[1,8,9]. Such a toolbox makes it possible to express physics using PDE's while keeping the geometric structures the quantities are related to. In differential geometry the operators grad, curl and div are replaced by a single exterior derivative that operates on different kinds of forms and the previously mentioned theorems are replaced by the generalized Stokes' theorem.
In order to have an appropriate discretization, these properties must also hold for the discretization, so the action of the generalized Stokes theorem and the exterior dervative must be satisfied exactly in the discrete case. Both exact discrete analogues are important to ensure conservation in conservation laws. The discretization used here is based on *algebraic topology*[12,15], that is the discrete counterpart of differential geometry. The theory of algebraic topology is based on chains and cochains, where the former represents the geometric object (e.g. points, lines, surfaces and volumes) and the latter represents the discretized phyical quantity that lives on the chain, i.e. a cochain is the discrete counterpart of a differential form.
In this work we focus on the discretization of boundary value problems for the convection-diffusion equation

$$-\epsilon\Delta\alpha + \mathbf{v}\cdot\nabla\alpha = f \quad \text{in } \Omega \subset \mathbb{R}^n, \tag{1}$$

and the diffusive and convective sub-problems, the Poisson equation and the linear convection equation. By expressing the convection-diffusion equation in terms of differential forms, it turns out that there exists a whole family of convection-diffusion equations given by

$$-\epsilon(\star\mathrm{d}\star\mathrm{d} + \mathrm{d}\star\mathrm{d}\star)\alpha^{(k)} + \mathcal{L}_{\mathbf{v}}\alpha^{(k)} = f^{(k)} \quad \text{in } \Omega \subset \mathbb{R}^n, \tag{2}$$

with unknown k-form $\alpha^{(k)}$, $0 \leq k \leq n$. The symbol $\star$ is the metric dependent Hodge-$\star$ operator, d the purely topological exterior derivative operator and $\mathcal{L}_{\mathbf{v}}$ the Lie-derivative, representing the convective part.
The mimetic framework sketched here, and explained in more detail in the next section, is combined with the spectral element method. Suitable polynomial basis-functions are chosen that mimic the geometric properties and are able to interpolate the cochains expressed on the different geometric objects. The basis-functions used are the Lagrange polynomials and edge polynomials[10,14], to interpolate values in points and line elements. Using tensor products, any geometric object can be interpolated and since edge polynomials are 1-forms, any degree of differential form can be constructed.
The outline of the paper is as follow: Section 2 introduces the mimetic framework, it gives an introduction in differential geometry and algebraic topology and their connection. In Section 3 properties of the mimetic polynomials are given and the mimetic spectral element method is explained for the Poisson equation and a convection equation and some numerical examples are given. Finally, some numerical examples of convection-diffusion problems are shown. Section 4 concludes this work and some remarks for future steps are made.

2 MIMETIC FRAMEWORK

This section explaines the basics of the mimetic framework used, that is based on differential geometry for the formulation of the PDE's in continuous space and on algebraic topology for their discrete counterpart. Finally the connection between the two is discussed.

2.1 Differential geometry

Here an introductory overview is given on differential geometry. This subsection is largely based on books of Abraham[1], Flanders[8] and Frankel[9]. The authors refer to these for more detail about differential geometry.

Differential forms

In (2) the unknown $\alpha^{(k)}$ is a *differential form* of degree k, a k-form. A k-form $\alpha^{(k)} \in \Lambda^k(\Omega)$ is a k-linear, antisymmetric tensor field over Ω. As an example, the velocity in $\mathbb{R}^3$ is a 1-form given by the expression

$$u^{(1)} = u(x,y,z)\mathrm{d}x + v(x,y,z)\mathrm{d}y + w(x,y,z)\mathrm{d}z. \tag{3}$$

Now consider two differential forms, a k-form and an l-form. In differential geometry there exists a *wedge product*, $\wedge : \Lambda^k(\Omega) \times \Lambda^l(\Omega) \mapsto \Lambda^{k+l}(\Omega)$, $k+l \leq n$, such that the product of the two forms produce a $(k+l)$-form. The wedge product is an anti-symmetric operator, i.e. $\alpha^{(k)} \wedge \alpha^{(k)} = 0$ and $\alpha^{(k)} \wedge \beta^{(l)} = -\beta^{(l)} \wedge \alpha^{(k)}$.

The second operator to be introduced is the *exterior derivative*, $\mathrm{d} : \Lambda^k(\Omega) \mapsto \Lambda^{k+1}(\Omega)$. It is defined using the *generalized Stokes' theorem*: let Ω_{k+1} be a $(k+1)$-dimensional manifold and $\alpha^{(k)} \in \Lambda^k(\Omega)$, then

$$\int_{\partial\Omega_{k+1}} \alpha^{(k)} = \int_{\Omega_{k+1}} \mathrm{d}\alpha^{(k)} \quad \Leftrightarrow \quad \langle \alpha^{(k)}, \partial\Omega_{k+1} \rangle = \langle \mathrm{d}\alpha^{(k)}, \Omega_{k+1} \rangle. \tag{4}$$

where $\partial\Omega_{k+1}$ is the k-dimensional space being the boundary of domain Ω_{k+1}. According to the duality pairing in (4), the exterior derivative is the formal adjoint of the *boundary operator* $\partial : \Omega_{k+1} \mapsto \Omega_k$. Applying the exterior derivative twice always leads to the null $(k+2)$-form, $\mathrm{d}(\mathrm{d}\alpha^{(k)}) = 0^{(k+2)}$. The exterior derivative gives rise to an exact sequence, called *De Rham complex*[2],

$$\mathbb{R} \hookrightarrow \Lambda^0(\Omega) \overset{\mathrm{d}}{\mapsto} \Lambda^1(\Omega) \overset{\mathrm{d}}{\mapsto} \Lambda^2(\Omega) \overset{\mathrm{d}}{\mapsto} \Lambda^3(\Omega) \overset{\mathrm{d}}{\mapsto} 0. \tag{5}$$

In vector calculus a similar sequence exists, where, from left to right for $\mathbb{R}^3$, the d's are replaced by the vector operators grad, curl and div. The exterior derivative is independent of any metric and coordinate system. The wedge product and exterior derivative are related using Leibniz's rule as

$$\mathrm{d}\left(\alpha^{(k)} \wedge \beta^{(l)}\right) = \mathrm{d}\alpha^{(k)} \wedge \beta^{(l)} + (-1)^k \alpha^{(k)} \wedge \mathrm{d}\beta^{(l)}, \quad \text{for } k+l < n. \tag{6}$$

Hodge-$\star$

All the metric and coordinate system dependency is in the *Hodge-$\star$ operator*, $\star : \Lambda^k(\Omega) \mapsto \Lambda^{n-k}(\Omega)$. Let $(\cdot,\cdot)$ be an inner-product for k-forms in terms of its vector proxies and let $\sigma^{(n)}$ be a normalized volume-form, then the Hodge-$\star$ operator is defined as

$$\left(\alpha^{(k)}, \beta^{(k)}\right) \sigma^{(n)} = \alpha^{(k)} \wedge \star\beta^{(k)}. \tag{7}$$

Alternatively we can write

$$\left(\star\alpha^{(k)}, \beta^{(n-k)}\right) \sigma^{(n)} = \alpha^{(k)} \wedge \beta^{(n-k)}, \tag{8}$$

and the corresponding variational form for the Hodge-$\star$, as will be used in a later section, is given by[1]

$$\left(\star\alpha^{(k)}, \beta^{(n-k)}\right)_\Omega = \int_\Omega \alpha^{(k)} \wedge \star\beta^{(n-k)} \tag{9}$$

An example of the Hodge-$\star$ operation in $\mathbb{R}^3$ for the orthonormal basis x, y, z is

$$\star\mathrm{d}x = \mathrm{d}y \wedge \mathrm{d}z, \quad \star\mathrm{d}y = \mathrm{d}z \wedge \mathrm{d}x, \quad \star\mathrm{d}z = \mathrm{d}x \wedge \mathrm{d}y. \tag{10}$$

[1] where $\left(\star\alpha^{(k)}, \beta^{(n-k)}\right)_\Omega \equiv \int_\Omega \left(\star\alpha^{(k)}, \beta^{(n-k)}\right) \sigma^{(n)}$

Applying the Hodge-$\star$ operator twice will either return the original k-form or with opposite sign,

$$\star\star\,\alpha^{(k)} = (-1)^{k(n-k)}\alpha^{(k)}. \tag{11}$$

The effect of the Hodge-$\star$ operator can be illustrated best as follows; take two De Rham complexes of (5) in opposite direction[7]. Then the connection is made by the Hodge-$\star$ operator, illustrated for $n = 3$ as

$$\begin{array}{ccccccccccc}
\mathbb{R} & \longrightarrow & \Lambda^0(\Omega) & \xrightarrow{\mathrm{d}} & \Lambda^1(\Omega) & \xrightarrow{\mathrm{d}} & \Lambda^2(\Omega) & \xrightarrow{\mathrm{d}} & \Lambda^3(\Omega) & \xrightarrow{\mathrm{d}} & 0 \\
 & & \star\updownarrow & & \star\updownarrow & & \star\updownarrow & & \star\updownarrow & & \\
0 & \xleftarrow{\mathrm{d}} & \tilde{\Lambda}^3(\Omega) & \xleftarrow{\mathrm{d}} & \tilde{\Lambda}^2(\Omega) & \xleftarrow{\mathrm{d}} & \tilde{\Lambda}^1(\Omega) & \xleftarrow{\mathrm{d}} & \tilde{\Lambda}^0(\Omega) & \longleftarrow & \mathbb{R}.
\end{array} \tag{12}$$

This dual De Rham complex clearly shows the paths to be taken for the Laplace-De Rham operator, $\star\mathrm{d}\star\,\mathrm{d} + \mathrm{d}\star\,\mathrm{d}\star$, for the diffusive part of the convection-diffusion equation (2). The dual De Rham complex in (12) will lead to a dual (staggered) grid method later on.

Lie-derivative

The convective part of (2) introduced the *Lie-derivative*, $\mathcal{L}_{\mathbf{v}} : \Lambda^k(\Omega) \mapsto \Lambda^k(\Omega)$. The Lie-derivative indicates how the k-form changes under the influence of a vector field $\mathbf{v} \in T(\Omega)$. The vector field $\mathbf{v}$ in $\mathbb{R}^3$ is given by

$$\mathbf{v} = v^1\frac{\partial}{\partial x^1} + v^2\frac{\partial}{\partial x^2} + v^3\frac{\partial}{\partial x^3}. \tag{13}$$

Two well-known expressions of the convective derivative are that of a 0-form and an n-form. The first results in the advective form,

$$\mathcal{L}_{\mathbf{v}}\alpha^{(0)} = v^1\frac{\partial\alpha}{\partial x^1} + v^2\frac{\partial\alpha}{\partial x^2} + v^3\frac{\partial\alpha}{\partial x^3} \tag{14}$$

and the second in the conservative form. For $n = 3$ this is

$$\mathcal{L}_{\mathbf{v}}\alpha^{(3)} = \left(\frac{\partial(v^1\alpha)}{\partial x^1} + \frac{\partial(v^2\alpha)}{\partial x^2} + \frac{\partial(v^3\alpha)}{\partial x^3}\right)\mathrm{d}x^1\wedge\mathrm{d}x^2\wedge\mathrm{d}x^3. \tag{15}$$

The Lie-derivative can be expressed in terms of the exterior derivative and the (not yet defined) interior product using *Cartan's formula*[9] as

$$\mathcal{L}_{\mathbf{v}} = i_{\mathbf{v}}\mathrm{d} + \mathrm{d}i_{\mathbf{v}}. \tag{16}$$

The new operator is the *interior product*, $i_{\mathbf{v}} : \Lambda^k(\Omega) \mapsto \Lambda^{k-1}(\Omega)$. It is a contraction of a k-form $\alpha^{(k)}$ to a $(k-1)$-form due to a vector field $\mathbf{v}$ as

$$i_{\mathbf{v}}\alpha^{(k)}(\mathbf{w}_1,\ldots,\mathbf{w}_{k-1}) = \alpha^{(k)}(\mathbf{v},\mathbf{w}_1,\ldots,\mathbf{w}_{k-1}). \tag{17}$$

As an example, consider the action of vector field $\mathbf{v} = v^1 \frac{\partial}{\partial x} + v^2 \frac{\partial}{\partial y}$ to a 2-form $\mathrm{d}x \wedge \mathrm{d}y$,

$$\begin{aligned}(\mathrm{d}x \wedge \mathrm{d}y)(\mathbf{v}, \mathbf{w}) &= \begin{vmatrix} v^1 & v^2 \\ \mathrm{d}x(\mathbf{w}) & \mathrm{d}y(\mathbf{w}) \end{vmatrix} \\ &= v^1 \mathrm{d}y(\mathbf{w}) - v^2 \mathrm{d}x(\mathbf{w}) \\ &= (-v^2 \mathrm{d}x + v^1 \mathrm{d}y)(\mathbf{w}). \end{aligned} \tag{18}$$

So the result of the contraction is the 1-form $-v^2 \mathrm{d}x + v^1 \mathrm{d}y$. A more extensive discussion about vector fields and Lie derivative can be found in Palha et. al.[13].

Mapping

Discretizations can often easily be expressed on orthogonal grids in rectangular domains. Domains of interest however have often a more exotic shape. Therefore the following mapping is introduced; given a reference domain Ω_0 with coordinates $\xi^1, \ldots, \xi^m$ and a physical domain Ω with $x^1, \ldots, x^n$, there exists a smooth mapping $\phi : \Omega_0 \mapsto \Omega$. This mapping introduces a mapping of differential forms in opposite direction, $\phi^\star : \Lambda^k(\Omega) \mapsto \Lambda^k(\Omega_0)$, called the *pullback operator*. The mapping is such that for all $\alpha^{(k)} \in \Lambda^k(\Omega)$ it holds that

$$\int_{\phi(\Omega_0)} \alpha^{(k)} = \int_{\Omega_0} \phi^\star \alpha^{(k)}. \tag{19}$$

For the current work, we need two more properties of the pullback operator:

(i). It commutes with the exterior derivative: $\mathrm{d}\left(\phi^\star \alpha^{(k)}\right) = \phi^\star \left(\mathrm{d}\alpha^{(k)}\right)$;

(ii). It is an algebraic homomorphism: $\phi^\star \left(\alpha^{(k)} \wedge \beta^{(l)}\right) = \left(\phi^\star \alpha^{(k)}\right) \wedge \left(\phi^\star \beta^{(l)}\right)$.

The mapping ϕ also induces a mapping of vector fields, $\phi_\star : T(\Omega_0) \mapsto T(\Omega)$, called the *push forward operator*, so that if $\mathbf{v} \in T(\Omega_0)$, then $\phi_\star \mathbf{v} \in T(\Omega)$. This shows that the action of $\phi^\star$ on the contraction of a k-form by $\mathbf{v}$ is given by

$$\phi^\star \left(i_{\phi_\star \mathbf{v}} \alpha^{(k)}\right) = i_{\mathbf{v}} (\phi^\star \alpha^{(k)}). \tag{20}$$

2.2 Algebraic topology

Algebraic topology describes the relations between different geometric objects using algebraic relations, without considering the concepts of distances and measures. Algebraic topology is the discrete counterpart of differential geometry, it mimics its properties on a discrete structure. For a more extensive discussion on algebraic topology applied in this field, see[12,15].

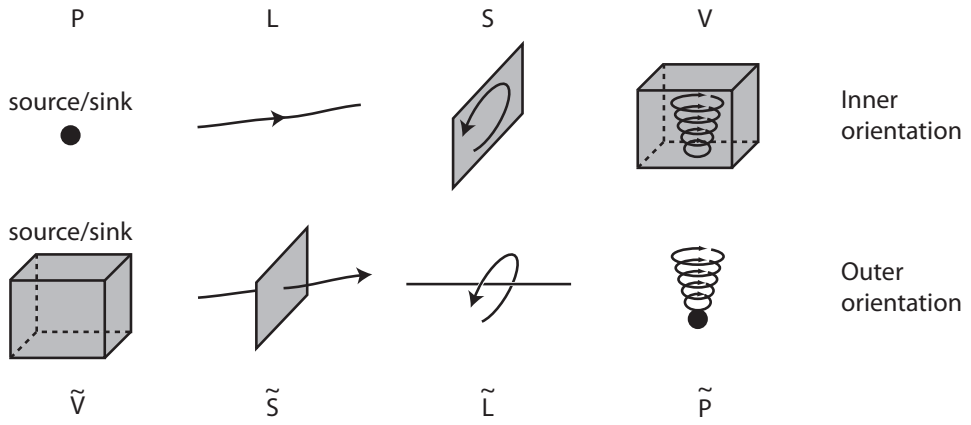

Figure 1: Inner and outer orientations for objects in $\mathbb{R}^3$.

Geometry and chains

Let's consider for the moment $\mathbb{R}^3$, we can distinguish four geometrical objects, i.e. points, lines, surfaces and volumes (in a mesh they are often called vertices, edges, faces and 3D-cells). In algebraic topology, these geometric objects are called *k-cells*, τ_k, $k = 0, 1, 2, 3$ in $\mathbb{R}^3$. The collection of all k-cells is called a *k-chain*, $\mathbf{c}_k \in C_k(D)$, and the collection of all k-chains is called a *cell-complex*, D. All k-cells have an *orientation*. We can associate two kind of orientations to each k-cell, either an inner or an outer orientation. This is illustrated in figure 1. Note the similarity with (12).

The outer oriented k-cells belong to the *primal* cell-complex D, while the inner oriented k-cells form the *dual* cell-complex $\tilde{D}$. From the way the primal cell complex has been defined, it follows that to every k-cell of D there corresponds a $(n-k)$-cell of $\tilde{D}$.

The k-cells in a k-chain are numbered and oriented and are written as a formal sum,

$$\mathbf{c}_k = \sum_{i=1}^{n_k} w_i \tau_k^i, \quad \text{with } w_i \in [-1, 0, 1], \tag{21}$$

where the value w_i indicates whether a cell is part of the chain and if it is defined in the same or opposite direction. The boundary $\partial\tau_k$ of a k-cell τ_k are $(k-1)$-cells, τ_{k-1}, called the *faces* of the k-cells. Then the boundary of a k-chain is the weighted sum of the boundaries of the k-cells,

$$\partial \mathbf{c}_k = \partial \left(\sum_{i=1}^{n_k} w_i \tau_k^i \right) = \sum_{i=1}^{n_k} w_i \partial \tau_k^i. \tag{22}$$

This operator $\partial : C_k(D) \mapsto C_{k-1}(D)$ is called the *boundary operator*. It can be proven that for any k-chain $\mathbf{c}_k$ it holds that the boundary of the boundary of a k-chain is empty, so

$$\partial(\partial \mathbf{c}_k) = 0. \tag{23}$$

With this boundary operator an exact sequence can be given as

$$0 \xleftarrow{\partial} C_0 \xleftarrow{\partial} C_1 \xleftarrow{\partial} C_2 \xleftarrow{\partial} C_3 \leftarrow 0. \tag{24}$$

Now consider those $(k+1)$-cells that have a k-cell as common boundary, called the *cofaces* of a k-cell. We can set up an *incidence matrix*, $\mathsf{E}_{(k+1,k)}$, relating the k-cells with its cofaces, by taking the i^{th} $(k+1)$-cell τ^i_{k+1} and the j^{th} k-cell τ^j_k in the complex,

$$\begin{aligned}\left(\mathsf{E}_{(k+1,k)}\right)_{i,j} &= \left[\tau^i_{k+1}, \tau^j_k\right] \\ &= \begin{cases} 0 & \text{if } \tau^j_k \text{ is not a face of } \tau^i_{k+1}, \\ 1 & \text{if } \tau^j_k \text{ is a face of } \tau^i_{k+1} \text{ with the same orientation}, \\ -1 & \text{if } \tau^j_k \text{ is a face of } \tau^i_{k+1} \text{ with the opposite orientation}. \end{cases}\end{aligned} \tag{25}$$

Incidence matrices can also be set up for associated dual cell complexes, $\tilde{\mathsf{E}}_{(k+1,k)}$. If the same index is assigned to pairs of dual cells the following relation holds:

$$\tilde{\mathsf{E}}_{(k+1,k)} = -\mathsf{E}^T_{(n-k,n-k-1)}. \tag{26}$$

Later we will see that these incidence matrices can in fact be used as discrete gradient, curl and divergence matrices.

Fields and cochains

Now consider a physical domain Ω which is subdivided into a cell complex D. The fields $\mathcal{F}$ of interest will manifest themselves as collections of global quantities associated with the cells in the cell complex. There is a function $\mathbf{c}^k \in C^k(D)$ which assigns to each τ^i_k of D an element c^i of $\mathcal{F}$,

$$\langle \tau^i_k, \mathbf{c}^k \rangle = c^i. \tag{27}$$

where $\langle \cdot, \cdot \rangle$ denotes a duality pairing. This function $\mathbf{c}^k : C_k(D) \mapsto \mathcal{F} \in \mathbb{R}$, called a *cochain*, is a linear mapping which assigns to each chain $\mathbf{c}_k$ a value $\langle \mathbf{c}_k, \mathbf{c}^k \rangle \in \mathbb{R}$, as

$$\left\langle \mathbf{c}_k, \mathbf{c}^k \right\rangle \equiv \int_{\mathbf{c}_k} \mathbf{c}^k. \tag{28}$$

This duality pairing can also be written as

$$\langle \mathbf{c}_k, \mathbf{c}^k \rangle = \left\langle \sum_{i=1}^{n_k} w_i \tau^i_k, \mathbf{c}^k \right\rangle = \sum_{i=1}^{n_k} w_i \left\langle \tau^i_k, \mathbf{c}^k \right\rangle = \sum_{i=1}^{n_k} w_i c^i. \tag{29}$$

With the introduction of cochains, topological laws containing fields can be expressed in a discrete form. The discrete relations will equate a global physical quantity associated

with a geometric object to another global quantity associated with the boundary of the former.
Let us define an operator δ, that transforms a k-cochain $\mathbf{c}^k$ into a $(k+1)$-cochain, $\delta\mathbf{c}^k$, by the following relation:

$$\langle \mathbf{c}_{k+1}, \delta\mathbf{c}^k \rangle \stackrel{\text{def}}{=} \langle \partial\mathbf{c}_{k+1}, \mathbf{c}^k \rangle. \tag{30}$$

This operator $\delta : C^k(D) \mapsto C^{k+1}(D)$ is called the *coboundary operator*. So the coboundary operator takes a quantity associated with the boundary of a geometric object and transfers it to the object itself. The coboundary operator can be seen as the discrete version of the exterior derivative, and so, it posesses the discrete version of the Poincaré Lemma, $\delta(\delta\mathbf{c}^k) = 0$. This follows directly from (30) and (23),

$$\langle \mathbf{c}_{k+2}, \delta\delta\mathbf{c}^k \rangle = \langle \partial\mathbf{c}_{k+2}, \delta\mathbf{c}^k \rangle = \langle \partial\partial\mathbf{c}_{k+2}, \mathbf{c}^k \rangle = \langle 0_{k+2}, \mathbf{c}^k \rangle = \mathbf{0}^{k+2}. \tag{31}$$

Like the exterior derivative in (5), also the coboundary operator gives rise to the following exact sequence,

$$0 \to C^0 \stackrel{\delta}{\to} C^1 \stackrel{\delta}{\to} C^2 \stackrel{\delta}{\to} C^3 \to 0. \tag{32}$$

The behavior of the coboundary operator reminds us on that of the incidence matrix. We can write

$$\langle \mathbf{c}_{k+1}, \delta\mathbf{c}^k \rangle = \langle \partial\mathbf{c}_{k+1}, \mathbf{c}^k \rangle = \mathsf{E}_{k+1,k}\mathbf{c}^k, \tag{33}$$

and it posesses the property of (31),

$$\langle \mathbf{c}_{k+2}, \delta\delta\mathbf{c}^k \rangle = \mathsf{E}_{k+2,k+1}\mathsf{E}_{k+1,k}\mathbf{c}^k = \mathbf{0}^{k+2}. \tag{34}$$

From (33) we observe that matrix $\mathsf{E}_{k+1,k}$ can be used as the matrix representation of the coboundary and thus be used as the discrete gradient, curl and divergence matrices.

2.3 Mimetic operators

The idea of a mimetic framework is that the discrete expression of the problem has the same mathematical properties as the continuous one. Two operators will be introduced which define the relation between the continuous differential forms and discrete cochains, being the reduction operator $\mathcal{R}$ and the reconstruction operator $\mathcal{I}$. Both operators posses a commuting property, revealing the unique relation between the exterior derivative and the coboundary operator. The ideas of the mimetic framework presented here is largely based on the work of Bochev and Hyman[3].

The *reduction operator* $\mathcal{R} : \Lambda^k(\Omega) \mapsto C^k(D)$ maps differential forms to cochains. This map is called the *De Rham map* and is defined by

$$\langle \mathcal{R}\alpha^{(k)}, \mathbf{c}_k \rangle = \int_{\mathbf{c}_k} \alpha^{(k)}. \tag{35}$$

A nice and useful property of the De Rham map is the *commuting diagram property* (CDP1)[3],

$$\mathcal{R}\mathrm{d} = \delta\mathcal{R}. \tag{36}$$

This property can be proven using Stokes' theorem (4) and the duality property of (30),

$$\langle \mathcal{R}\mathrm{d}\alpha^{(k)}, \mathbf{c}_k \rangle = \int_{\mathbf{c}_k} \mathrm{d}\alpha^{(k)} = \int_{\partial \mathbf{c}_k} \alpha^{(k)} = \langle \mathcal{R}\alpha^{(k)}, \partial \mathbf{c}_k \rangle = \langle \delta\mathcal{R}\alpha^{(k)}, \mathbf{c}_k \rangle. \tag{37}$$

The reconstruction operator $\mathcal{I} : C^k(D) \mapsto \Lambda^k(\Omega)$, called the *Whitney map*, maps cochains back to differential forms. Where the reduction step has a clear definition (35), the reconstruction step $\mathcal{I}$ is free to choose. This is where methods like FD, FV and FE differ from each other. Although the choice of a reconstruction method is free, $\mathcal{I}$ must satisfy the following two properties: $\mathcal{I}$ must be the right inverse of $\mathcal{R}$, so it returns identity (*consistency property*)

$$\mathcal{R}\mathcal{I} = Id \tag{38}$$

and its left inverse must be an approximation, so the result is close to identity (*approximation property*)

$$\mathcal{I}\mathcal{R} = Id + \mathcal{O}\left(h^a\right). \tag{39}$$

The operator $\mathcal{I}\mathcal{R}$ makes it possible to give an approximate continuous representation of a k-form $\alpha^{(k)}$,

$$\alpha^{(k)} \approx \alpha_h^{(k)} = \mathcal{I}\mathcal{R}\alpha^{(k)}, \tag{40}$$

where $\mathcal{I}\mathcal{R}\alpha^{(k)}$ is expressed as a combination of k-cochains and interpolating k-forms. The reconstruction operator $\mathcal{I}$ also satisfies a commuting diagram property (CDP2),

$$\mathrm{d}\mathcal{I} = \mathcal{I}\delta. \tag{41}$$

Properties like (36) and (41) are typical for conforming and mimetic methods.

3 MIMETIC SPECTRAL ELEMENT METHOD

Now that a nice mimetic framework is formulated, we seek for a discretization method that satisfy all the properties of the mimetic framework. First the polynomials with mimetic properties are described. Next the discretization is exprained using different kinds of sample problems.

3.1 Mimetic polynomials

In spectral element methods functions are approximated using a polynomial expansion. Consider a function $\alpha(\xi)$, expanded using *Lagrange polynomials*, then

$$\begin{aligned} \alpha(\xi) &= \sum_{i=0}^{\infty} \alpha(\xi_i) h_i(\xi) \\ &\approx \sum_{i=0}^{N} \alpha(\xi_i) h_i(\xi). \end{aligned} \tag{42}$$

The function $\alpha(\xi)$ is approximated by a N^{th}-order polynomial $\alpha_h(\xi)$. Suppose that $\alpha(\xi)$ represents a potential, which is a 0-form, $\alpha^{(0)}(\xi)$, then $\alpha(\xi_i)$ can be considered as the reduction of $\alpha^{(0)}(\xi)$, being an element of a 0-cochain. So alternatively (42) can be written as

$$\alpha^{(0)}(\xi) \approx \mathcal{I}\mathcal{R}\alpha^{(0)}(\xi) = \alpha_h^{(0)}(\xi) = \sum_{i=0}^{N} \alpha(\xi_i) h_i(\xi). \tag{43}$$

So Lagrange polynomials are able to reconstruct a 0-form from a 0-cochain. Lagrange polynomials have the nice property that its value is one in the corresponding point and zero in all other mesh points (see figure 2),

$$\mathcal{R}h_i(\xi) = h_i(\xi_p) = \begin{cases} 1 & \text{if } i = p \\ 0 & \text{if } i \neq p \end{cases}. \tag{44}$$

Lagrange polynomials are in fact 0-forms themselves, $h_i^{(0)}(\xi)$. Robidoux[14] and Gerritsma[10] developed polynomials that have similar properties for 1-forms, $e_i^{(1)}(\xi)$. Take the external derivative of $\alpha^{(0)}(\xi)$, it gives the 1-form $u^{(1)}(\xi)$ by

$$\begin{aligned} u^{(1)}(\xi) = \mathrm{d}\alpha^{(0)}(\xi) &\approx \mathrm{d}\left(\sum_{i=0}^{N} \alpha(\xi_i) h_i^{(0)}(\xi) \right) \\ &= \sum_{i=0}^{N} \alpha(\xi_i) \mathrm{d}h_i^{(0)}(\xi) \\ &= \sum_{i=1}^{N} (\alpha(\xi_i) - \alpha(\xi_{i-1})) \left[-\sum_{k=0}^{i-1} \mathrm{d}h_k^{(0)}(\xi) \right] \\ &= \sum_{i=1}^{N} u_i e_i^{(1)}(\xi). \end{aligned} \tag{45}$$

The cochain corresponding to line segment (1-cell) i is given by $u_i = \alpha_i - \alpha_{i-1}$. This is actually a discrete gradient operation in 1D. This operation is purely topological, no metric or coordinate system is involved. The polynomial $e_i^{(1)}(\xi)$ is called *edge polynomial*, it is a 1-form, given by

$$e_i^{(1)}(\xi) = -\sum_{k=0}^{i-1} \mathrm{d}h_k^{(0)}(\xi). \tag{46}$$

For convenience and to show the 1-form property, this can be written as

$$e_i^{(1)}(\xi) = \varepsilon_i(\xi)\mathrm{d}\xi, \quad \text{with} \quad \varepsilon_i(\xi) = -\sum_{k=0}^{i-1} \frac{\mathrm{d}h_k}{\mathrm{d}\xi}.$$

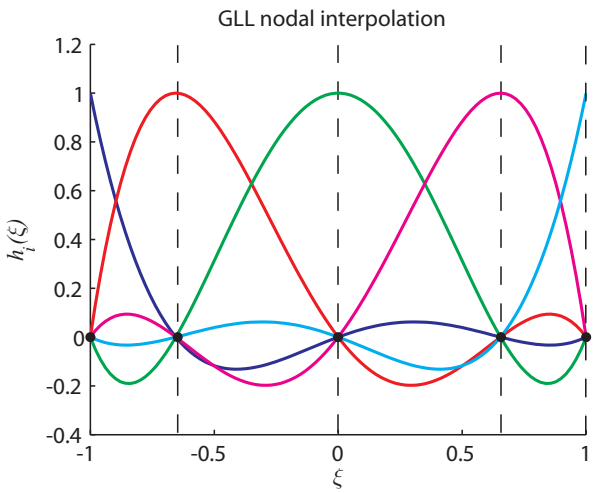

Figure 2: Lagrange polynomials on Gauss-Lobatto-Legendre grid.

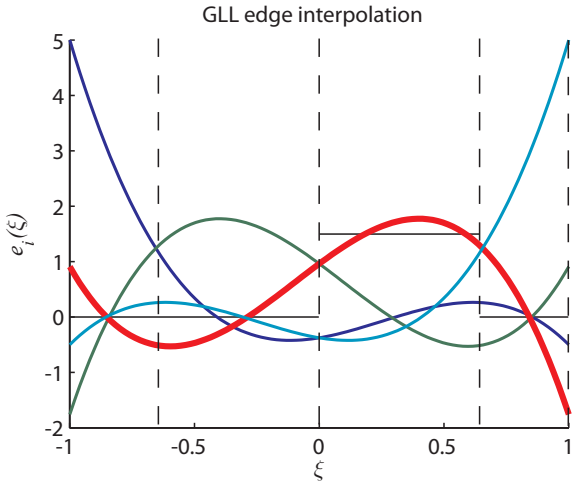

Figure 3: Edge polynomials on Gauss-Lobatto-Legendre grid.

Similar to (44), the edge polynomial has the special property when integrating the polynomial $e_i^{(1)}(\xi)$ over a line segment we get one for the corresponding element and zero for any other line segment, so

$$\mathcal{R}e_i^{(1)}(\xi) = \int_{\xi_{p-1}}^{\xi_p} e_i^{(1)}(\xi) = \begin{cases} 1 & \text{if } i = p \\ 0 & \text{if } i \neq p \end{cases}. \tag{47}$$

The Lagrange and edge polynomails are shown in figures 2 and 3. Now that Lagrange polynomials and edge polynomials are defined, we can construct interpolants for all the geometric objects using tensor products.

3.2 Mimetic spectral element method for Poisson equation

The implementation of the mimetic spectral element method is explained using a sample problem, the well-known Poisson equation.

Poisson equation in differential form

Consider the Poisson equation in $\mathbb{R}^3$ expressed using standard calculus as

$$\text{div}(\text{grad}\alpha) = f. \tag{48}$$

This equation can be written as a system of first-order relations

$$\text{grad}\alpha = \mathbf{u}, \quad \text{div}\mathbf{q} = f, \tag{49a}$$

with corresponding constitution relation

$$\mathbf{u} = \mathbf{q}. \tag{49b}$$

Instead of writing the system in vector form, we prefer to use differential forms of dimension n,

$$\mathrm{d}\alpha^{(0)} = u^{(1)}, \quad \mathrm{d}q^{(n-1)} = f^{(n)}. \tag{50a}$$

with as constitutive relation

$$\star u^{(1)} = q^{(n-1)}. \tag{50b}$$

Then (48) becomes

$$\mathrm{d} \star \mathrm{d}\alpha^{(0)} = f^{(n)}. \tag{51}$$

The right hand side, $f^{(n)}$, is typically a body force, that is naturally associated with a volume. Besides, $\alpha^{(0)}$ is a potential and $u^{(1)}$ and $q^{(n-1)}$ can interpreted as a velocity and a flux respectively. The last two are associated with different geometric object, which is unclear when looking at (49b).

Primal and dual mesh

Let's consider for the moment that the physical domain is equal to the reference element, $\Omega \equiv \Omega_0$ and thus $\phi = \phi^\star = Id$. Details on the derivation of the Poisson equation for curvilinear meshes can be found in Bouman et. al.[6]. As explained before, two cell complexes are needed for the calculations. The cochains of the fluxes and body forces are outer oriented cochains and thus are defined on the primal mesh, $(\xi^1, \ldots, \xi^n)$, and the potential and velocity cochains are inner oriented cochains and are therefore defined on the dual mesh,$(\tilde{\xi}^1, \ldots, \tilde{\xi}^n)$.

We choose to use a spectral element method for the reconstruction $\mathcal{I}$. The primal mesh within each spectral element consists of a *Gauss-Lobatto* mesh (GL) and the *Extended Gauss* mesh (EG) will be used for the dual mesh. The EG method is based on the standard Gauss collocation points and is extended with the two boundary points $\xi = \pm 1$, needed for the inter-element connectivity. Figure 4 shows a two-dimensional ($n = 2$) standard element with the two meshes, for $N = 3$, where N indicates the number of cells in horizontal and vertical direction.

Divergence on primal grid

Consider the right equation of (50a), the divergence relation. The diffusive flux $q^{(n-1)}$ is associated with the primal grid and is expressed as

$$\mathcal{I}\mathcal{R}q^{(1)}(\xi,\eta) = -\sum_{i=1}^{N}\sum_{j=0}^{N} q^{\eta}_{i,j} e_i(\xi) h_j(\eta) + \sum_{i=0}^{N}\sum_{j=1}^{N} q^{\xi}_{i,j} h_i(\xi) e_j(\eta), \tag{52}$$

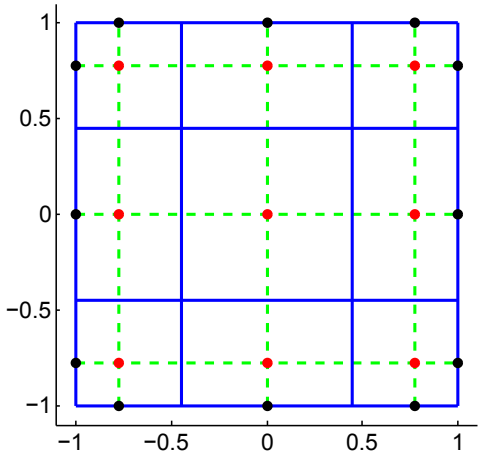

Figure 4: Primal (GL) mesh is given in blue, dual (EG) mesh in green, red (interior) and black (inter-element connectivity) dots are the unknowns potentials.

where the 1-cells $q^{\xi}_{i,j}$ and $q^{\eta}_{i,j}$ are the normal flux components in ξ and η direction. Apply the exterior derivative to (52) as in (50a) gives the 2-form

$$\begin{aligned}
\mathrm{d}\mathcal{I}\mathcal{R}q^{(1)}(\xi,\eta) &= -\sum_{i=1}^{N}\sum_{j=0}^{N} q^{\eta}_{ij} e_i(\xi)\mathrm{d}h_j(\eta) + \sum_{i=0}^{N}\sum_{j=1}^{N} q^{\xi}_{ij}\mathrm{d}h_i(\xi)e_j(\eta) \\
&= \sum_{i=1}^{N}\sum_{j=1}^{N}\left(q^{\xi}_{i,j} - q^{\xi}_{i-1,j} + q^{\eta}_{i,j} - q^{\eta}_{i,j-1}\right) e_i(\xi)e_j(\eta) \\
&\overset{(41)}{=} \mathcal{I}\delta\mathcal{R}q^{(1)} \overset{(36)}{=} \mathcal{I}\mathcal{R}\mathrm{d}q^{(1)},
\end{aligned} \tag{53}$$

So (41) is indeed satisfied and with (36) it reduces to the approximation of $\mathrm{d}q^{(1)}$. Let the body force $f^{(n)}$ be expressed as

$$\mathcal{I}\mathcal{R}f^{(2)}(\xi,\eta) = \sum_{i=1}^{N}\sum_{j=1}^{N} f_{i,j} e_i(\xi)e_j(\eta), \tag{54}$$

where $f_{i,j}$ are 2-cochains, then from the divergence relation (50a) we obtain

$$\sum_{i=1}^{N}\sum_{j=1}^{N}\left(q^{\xi}_{i,j} - q^{\xi}_{i-1,j} + q^{\eta}_{i,j} - q^{\eta}_{i,j-1} - f_{i,j}\right) e_i(\xi)e_j(\eta) = 0. \tag{55}$$

This shows that the cochains $\mathbf{q}^1$ are independent of the basis functions, $\mathcal{R}\mathrm{d}q^{(1)} = \delta\mathcal{R}q^{(1)} = \mathcal{R}f^{(2)}$, so

$$q^{\xi}_{i,j} - q^{\xi}_{i-1,j} + q^{\eta}_{i,j} - q^{\eta}_{i,j-1} = f_{i,j}, \quad \text{for } i,j = 1,\ldots,N, \tag{56}$$

and so the discrete divergence equation becomes

$$\mathsf{E}_{2,1}\mathbf{q}^1 = \mathbf{f}^2. \tag{57}$$

The result is a finite-volume formulation for the divergence equation. It can be shown that this is an exact, metric-free discretization[10].

Gradient on dual grid

Now consider the left relation of (50a). The 0-form $\alpha^{(0)}$ is expressed on the dual grid, as[2]

$$\tilde{\mathcal{I}}\tilde{\mathcal{R}}\alpha^{(0)}(\xi,\eta) = \sum_{i=1}^{N}\sum_{j=1}^{N}\alpha_{i,j}h_i^{\mathrm{G}}(\xi)h_j^{\mathrm{G}}(\eta). \tag{58}$$

Here $h_i^{\mathrm{G}}(\xi)$ are the Lagrange polynomials through the Gauss points and $h_i^{\mathrm{EG}}(\xi)$ those through the extended Gauss points. The velocity is found by applying the exterior derivative,

$$\begin{aligned}
\mathrm{d}\tilde{\mathcal{I}}\tilde{\mathcal{R}}\alpha^{(0)} &= \sum_{i=2}^{N}\sum_{j=1}^{N}(\alpha_{i,j}-\alpha_{i-1,j})e_i^{\mathrm{G}}(\xi)h_j^{\mathrm{G}}(\eta) + \sum_{i=1}^{N}\sum_{j=2}^{N}(\alpha_{i,j}-\alpha_{i,j-1})h_i^{\mathrm{G}}(\xi)e_j^{\mathrm{G}}(\eta) \\
&= \sum_{i=1}^{N+1}\sum_{j=1}^{N}(\alpha_{i,j}-\alpha_{i-1,j})e_i^{\mathrm{EG}}(\xi)h_j^{\mathrm{G}}(\eta) + \sum_{i=1}^{N}\sum_{j=1}^{N+1}(\alpha_{i,j}-\alpha_{i,j-1})h_i^{\mathrm{G}}(\xi)e_j^{\mathrm{EG}}(\eta) \\
&\overset{(41)}{=} \tilde{\mathcal{I}}\delta\tilde{\mathcal{R}}\alpha^{(0)} \overset{(36)}{=} \tilde{\mathcal{I}}\tilde{\mathcal{R}}\mathrm{d}\alpha^{(0)} \overset{(50a)}{=} \tilde{\mathcal{I}}\tilde{\mathcal{R}}u^{(1)}.
\end{aligned} \tag{59}$$

Again the second commuting diagram property (41) is satisfied. The reduced gradient relation becomes $\tilde{\mathcal{R}}\mathrm{d}\alpha^{(0)} = \delta\tilde{\mathcal{R}}\alpha^{(0)} = \tilde{\mathcal{R}}u^{(1)}$, and in matrix form this is

$$\mathbf{u}^1 = \tilde{\mathsf{E}}_{1,0}\mathbf{a}^0, \tag{60}$$

where $\mathbf{u}^1$ and $\mathbf{a}^0$ are the velocity 1-cochain and the potential 0-cochain respectively. Again this equation is exact and metric-free.

Discrete Hodge-$\star$ operator

In the discussion of the discrete structures in section 2.2 there was no part about a discrete counterpart of the Hodge-$\star$ operator, $\mathsf{H} : C^k \mapsto C^{n-k}$. In fact there is no uniform definition of the discrete Hodge-$\star$ operator. In Bochev and Hyman[3], definitions for a *natural* and *derived* discrete Hodge-$\star$ operator are given. Because the Hodge-$\star$ operator

[2]The symbol $\tilde{}$ indicates the dual grid.

can only be performed in continuous space, in the natural definition, the cochains are first interpolated to forms and, after applying the Hodge-$\star$, reduced back to cochains,

$$\mathsf{H} = \mathcal{R} \star \mathcal{I}. \tag{61}$$

In practice this might only be useful if the dual grid is identical to the primal grid. Here we have a staggered grid. Alternatively, for any $a_h^{(k)}, b_h^{(k)} \in \Lambda^k(\Omega)$, a discrete Hodge-$\star$ can be derived using (9) as

$$\begin{aligned} \int_\Omega a_h^{(k)} \wedge b_h^{(k)} &= \left(\star a_h^{(k)}, b_h^{(k)} \right)_\Omega \\ &= \left(\mathcal{I} \mathsf{H} \mathbf{a}^k, b_h^{(k)} \right)_\Omega . \end{aligned} \tag{62}$$

The idea of the latter is adopted to make a connection between $u^{(1)}$ defined on the primal grid and $q^{(n-1)}$ defined on the dual grid,

$$\left(\star u_h^{(1)}, q_h^{(1)} \right)_\Omega = \int_\Omega u_h^{(1)} \wedge q_h^{(1)} \tag{63a}$$

$$\overset{(6)}{=} \int_{\partial\Omega} \alpha_h^{(0)} \wedge q_h^{(1)} - \int_\Omega \alpha_h^{(0)} \wedge \mathrm{d} q_h^{(1)}. \tag{63b}$$

The last step makes use of the Leibniz rule (6) to make a distinction between the interior part and boundary part of domain Ω as was done for the dual grid. Equation (63b) is also known as the *support operator method* proposed by Hyman[11].

3.3 Numerical examples for Poisson equation

Example 1: Single-element grid

The first test case is to solve (48) on $(x, y) \in [-1, 1]^2$, with

$$f(x, y) = -2m^2\pi^2 \sin(m\pi x) \sin(m\pi y) \tag{64}$$

and with appropriate Dirichlet or Neumann boundary conditions, such that the solution becomes

$$\alpha(x, y) = \sin(m\pi x) \sin(m\pi y). \tag{65}$$

In this testcase the boundary of the domain remains a square, but the interior is deformed. The following mapping ϕ is used with c as variable parameter

$$\begin{aligned} x(\xi, \eta) &= \xi + c\sin(\pi\xi)\sin(\pi\eta) \\ y(\xi, \eta) &= \eta + c\sin(\pi\xi)\sin(\pi\eta), \end{aligned} \tag{66}$$

Grids for $c = 0.0,\ 0.2,\ 0.3$ are shown in figure 5. The convergence of the potential and the flux for frequencies $m = 1$ and $m = 3$ are shown in figure 6. Although the exponential convergence rate is decreases for increasing grid curvature, the convergence remains

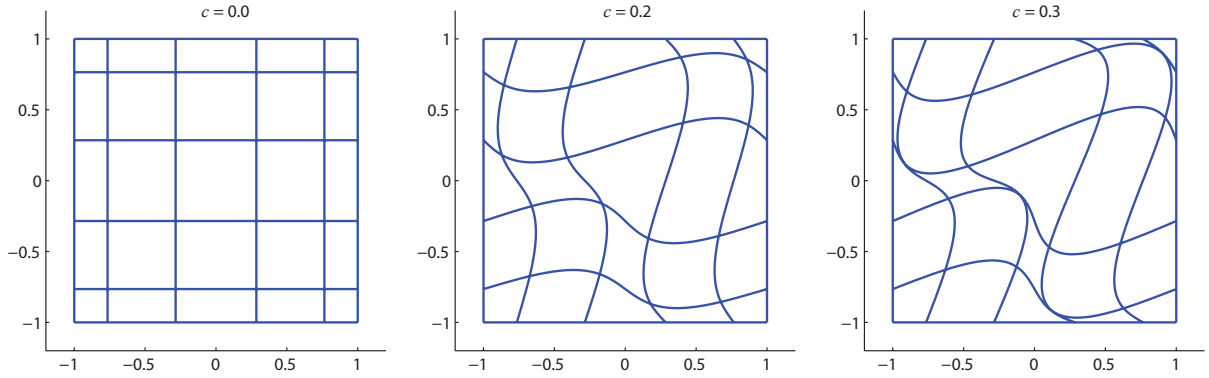

Figure 5: Deformed meshes for $N = 5$ and for $c = \{0.0,\ 0.2,\ 0.6\}$.

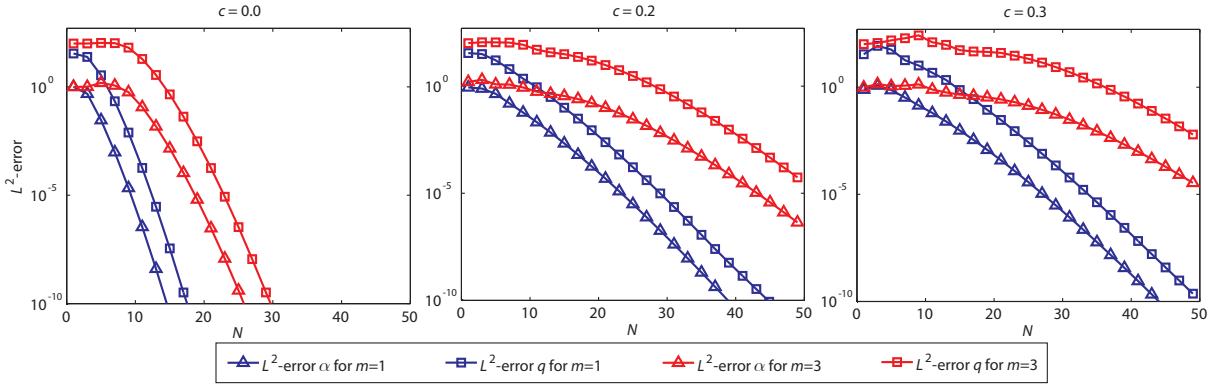

Figure 6: Convergence of $\alpha_h^{(0)}$ and $q_h^{(1)}$ on curved mesh $(c = 0.0, 0.2, 0.3)$ for $m = 1$ and $m = 3$.

exponential.

Example 2: Multi-element grid

The same problem is now solved on a uniform $(c = 0.0)$ and curved $(c = 0.2)$ multi-element grid to show the h- and p-convergence behaviour, see figure 7. For p-convergence we see again that the convergence rates decrease on curved grids, but remain exponential. For h-convergence the error increases in case of curved grids, however the linear convergence rate remain equal to the uniform case.

4 Mimetic spectral element method for convection equations

In section 2.1 the Lie-derivative was introduced as a convective derivative. It was expressed using Cartan's formula in terms of the exterior derivative and interior product. In this section we consider in $\mathbb{R}^2$ the convection of volume form $\alpha^{(2)} = \alpha(\xi, \eta)\mathrm{d}\xi \wedge \mathrm{d}\eta$,

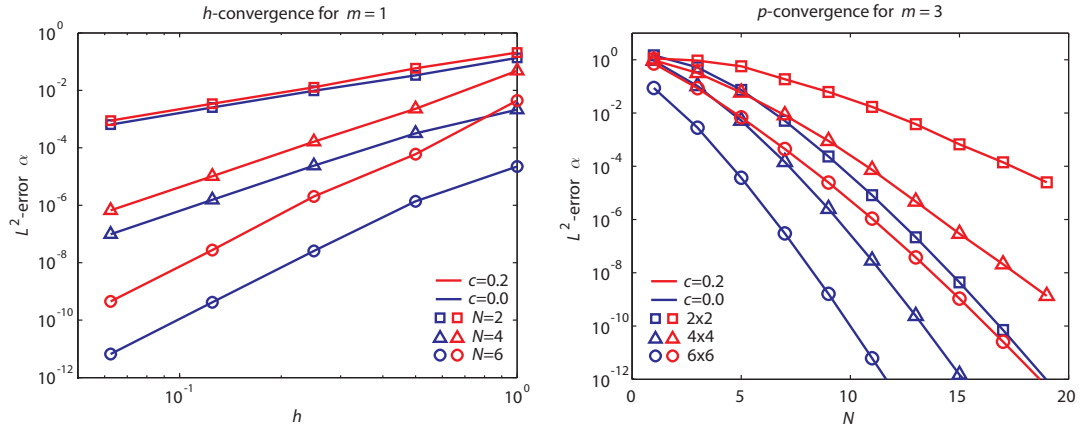

Figure 7: h- and p-convergence on uniform ($c = 0.0$) and curved ($c = 0.2$) multi-element grids.

with $\Omega = \Omega_0 = [-1, 1]^2$, so

$$\mathcal{L}_{\mathbf{v}}\alpha^{(2)} = 0, \quad \text{with } \mathbf{v} = v^1 \frac{\partial}{\partial \xi} + v^2 \frac{\partial}{\partial \eta}. \tag{67}$$

Because we consider a volume form in 2D, the Lie-derivative reduces to

$$\mathcal{L}_{\mathbf{v}}\alpha^{(2)} = \mathrm{d}i_{\mathbf{v}}\alpha^{(2)} = \mathrm{d}q^{(1)} = 0, \tag{68}$$

where here $q^{(1)}$ is the convective flux. The convective flux is given by

$$\begin{aligned} q^{(1)} &= i_X \alpha^{(2)} \\ &= -v^2 \alpha(\xi, \eta)\mathrm{d}\xi + v^1 \alpha(\xi, \eta)\mathrm{d}\eta \\ &= -q_\eta(\xi, \eta)\mathrm{d}\xi + q_\xi(\xi, \eta)\mathrm{d}\eta \end{aligned} \tag{69}$$

Now let's approximate $\alpha^{(2)}$ using outer-oriented 2-cochains and two edge functions defined on the primal grid as

$$\alpha_h^{(2)} = \sum_{i=1}^{N}\sum_{j=1}^{N} \alpha_{ij} e_i(\xi) e_j(\eta). \tag{70}$$

Then the action of the interior product results in

$$\begin{aligned} i_{\mathbf{v}}\alpha_h^{(2)} &= \sum_{i=1}^{N}\sum_{j=1}^{N} \alpha_{ij} \left(v^1 \varepsilon_i(\xi) e_j(\eta) - v^2 e_i(\xi) \varepsilon_j(\eta) \right) \\ &= -\sum_{i=1}^{N}\sum_{j=0}^{N} \underbrace{\left[v^2 \sum_{l=1}^{N} \alpha_{il} \varepsilon_l(\eta_j) \right]}_{=q^{\eta}_{i,j}} e_i(\xi) h_j(\eta) + \sum_{i=0}^{N}\sum_{j=1}^{N} \underbrace{\left[v^1 \sum_{k=1}^{N} \alpha_{kj} \varepsilon_k(\xi_i) \right]}_{q^{\xi}_{i,j}} h_i(\xi) e_j(\eta). \end{aligned} \tag{71}$$

The first line shows the resultant 1-form, because $\frac{\partial}{\partial \xi^i}(\mathrm{d}\xi^i) = 1$. However the basis-functions are different than that of the flux $q_h^{(1)}$. Therefore a transformation of basis-functions is needed as is done in the second line. Next step is applying the exterior derivative, this gives

$$\begin{aligned}\mathcal{L}_{\mathbf{v}}\alpha_h^{(2)} &= \mathrm{d}i_{\mathbf{v}}\alpha_h^{(2)} = \mathrm{d}q_h^{(1)} \\ &= \sum_{i=1}^{N}\sum_{j=1}^{N}\left(q_{ij}^{\xi} - q_{i-1j}^{\xi} + q_{ij}^{\eta} - q_{ij-1}^{\eta}\right) e_i(\xi)e_j(\eta).\end{aligned} \tag{72}$$

Because the Lie-derivative maps k-forms to k-forms both expressed on the same grid, it is independent of the basis-functions, in this case independent of $e_i(\xi)e_j(\eta)$. Therefore we can limit ourselves to the reduction of (72),

$$q_{ij}^{\xi} - q_{i-1j}^{\xi} + q_{ij}^{\eta} - q_{ij-1}^{\eta} = 0, \tag{73}$$

with the 1-cells $q_{i,j}^{\xi}$ and $q_{i,j}^{\eta}$ as defined in (71).

5 Numerical example for the convection equation

Example 3: Space-time convection of volume-form

In the first example, the convection equation (67) is solved for the space-time differential form $\alpha^{(2)} = \alpha(t,x)\mathrm{d}t \wedge \mathrm{d}x$ with vector field $\mathbf{v} = \frac{\partial}{\partial t} + a\frac{\partial}{\partial x}$ and periodic boundary conditions. The initial condition is $\alpha_{\mathrm{ic}}(x) = \frac{1}{2} - \frac{1}{2}\sin(2\pi x)$ for $-0.75 \leq x \leq 0.25$ and zero elsewhere. Figure 8 shows the solution of a single space-time spectral element for $a = 2$ with 30×30 unknowns. The polynomial order is 29 in both directions. In case of 2 periods per spectral element, figure 9 shows the solution after respectively 10^3 and 10^4 periods.

6 Numerical examples for the convection-diffusion equation

Example 4: The 1D single element grid, zero-form and volume form

This first example considers the following boundary value problem in 1D, with Pe the Peclet number as parameter,

$$Pe\frac{\partial \alpha}{\partial x} - \frac{\partial^2 \alpha}{\partial x^2} = 0, \tag{74a}$$

$$\alpha(0) = 1, \quad \alpha(1) = 0. \tag{74b}$$

The exact solution is given by

$$\alpha(x) = \frac{e^{Pe\cdot x} - e^{Pe}}{1 - e^{Pe}} \tag{75}$$

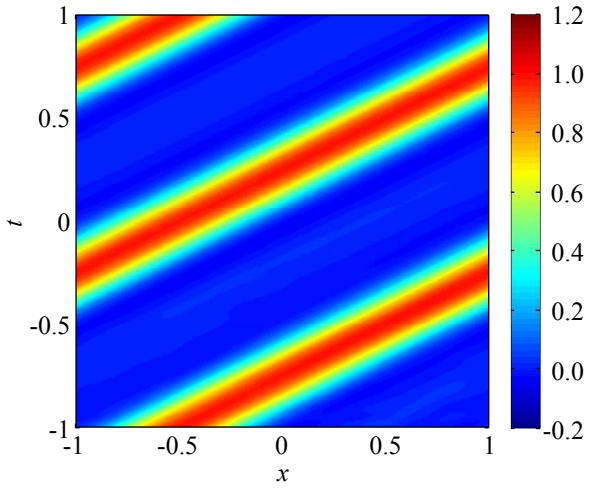

Figure 8: Space-time solution for $a = 2$ and $N = 30$.

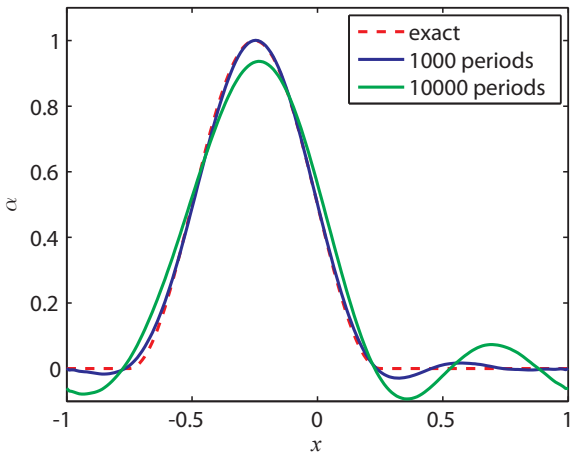

Figure 9: Exact vs. numerical solution after 10^3 and 10^4 periods.

This problem is solved for a zero-form $\alpha^{(0)}$ where (2) reduces to

$$i_{\mathbf{v}} \mathrm{d}\alpha^{(0)} + \star \mathrm{d} \star \mathrm{d}\alpha^{(0)} = 0, \tag{76a}$$

$$\alpha^{(0)}(0) = 1, \ \alpha^{(0)}(1) = 0, \tag{76b}$$

and also for a volume-form $\alpha^{(1)}$ where (2) reduces to

$$\mathrm{d} i_X \alpha^{(1)} + \mathrm{d} \star \mathrm{d} \star \alpha^{(1)} = 0, \tag{77a}$$

$$\star \alpha^{(1)} = 1 \text{ and } \star \alpha^{(1)}(1) = 0. \tag{77b}$$

In figure (6), the discrete and interpolated solutions are given for $Pe = 10$ and $N = 7$. Both solutions nicely follow the exact solution. Which one to chose depends in large amount on the physical quantity, e.g. a temperature field is usually expressed by a zero-form, while a consentration is associated with a volume-form.

7 CONCLUSIONS AND FUTURE WORK

In this paper a framework is described where the discretization method is kept as close as possible to the partial differential equations, i.e. it tries to mimic as much of the structures in the PDE's as possible. For that, the PDE's are expressed in terms of differential forms and the discretized system is given in terms of cochains. With the reduction and reconstruction operators the connections and similarities between the continuous and discrete operator are made clear. For the reconstruction, a spectral element method is described that satisfies the properties of the given framework. The mimetic spectral element method results in a method that is close to the finite volume method for the topological relations and becomes a higher-order finite element method for the metric

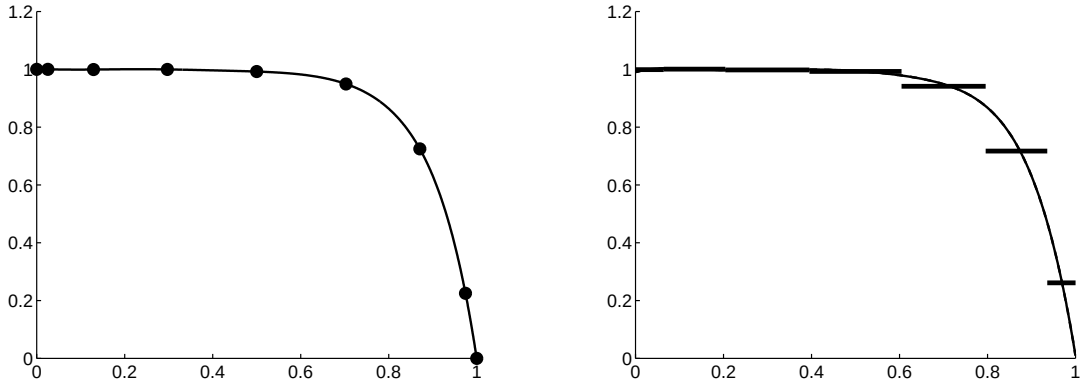

Figure 10: 1D convection-diffusion with $Pe = 10$ solved with point (left) and line elements (right) with their corresponding interpolations.

dependent part. The numerical examples discussed in the previous section indicate the possibilities of the method. As a future step we would like to investigate in more detail how well the method behaves.

References

[1] R. Abraham, J.E. Marsden and T. Ratiu. Manifolds, Tensor Analysis and Applications, *Applied Mathematical Sciences*, **75**, *Springer*, (2001)

[2] D.N. Arnold, R.S. Falk and R. Winther, Differential Complexes and Stability of Finite Element Methods I. The de Rham Complex. IMA **Vol. 142**, *Springer Verlag, eds.*, D. Arnold, P. Bochev, R. Lehoucq, R. Nicolaides and M. Shashkov, (2006).

[3] P.B. Bochev, J.M. Hyman, Principles of mimetic discretizations of differential operators. IMA **Vol. 142**, *Springer Verlag, eds.*, D. Arnold, P. Bochev, R. Lehoucq, R. Nicolaides and M. Shashkov, (2006).

[4] A. Bossavit, On the geometry of electromagnetism. *Journal of Japanese Society of Applied Electromagnetics and Mechanics* **6**, 17-28 (no 1), 114-23 (no 2), 233-40 (no 3), 318-26 (no 4), (1998).

[5] A. Bossavit, Computational electromagnetism and geometry: Building a finite-dimensional "Maxwell's house". *Journal of Japanese Society of Applied Electromagnetics and Mechanics*, **7**, 150-9 (no 1), 294-301 (no 2), 401-408 (no 3), and 8 (2000) 102-109 (no 4), 203-209 (no 5), 372-377 (no 6), (1999).

[6] M. Bouman, A. Palha, J. Kreeft and M. Gerritsma. A conservative spectral element method for curvilinear domains, *In prodeecings of ICOSAHOM 2009*, (2010).

[7] M. Desbrun, E. Kanso, Y. Tongy, Discrete Differential Forms for Computational Modeling, in proceedings of the *International conference on computer graphics and interactive techniques*, (2005)

[8] H. Flanders, Differential forms with applications to the physical sciences. *Dover publications*, (1989).

[9] T. Frankel, The geometry of physics, an introduction, *Cambridge University Press*, (2004).

[10] M.I. Gerritsma, Edge functions for spectral elements, *In prodeecings of ICOSAHOM 2009*, (2010).

[11] J. Hyman, M. Shaskov, S. Steinberg, The numerical solution of diffusion problems in strongly heterogeneous non-isentropic materials, *Journal of Comp. Physics*, **132**, 130-148, (1997).

[12] C. Mattiussi, A reference discretization strategy for the numerical solution of physical field problems, *Advances in imaging and electron physics*, **121**, 143-279 (2000).

[13] A. Palha, J. Kreeft and M. Gerritsma, Numerical solution of advection equations with the discretization of the Lie derivative, in proceedings of the *European conference on Computational Fluid Dynamics*, ECCOMAS CFD 2010, (2010).

[14] N. Robidoux, Polynomial Histopolation, Superconvergent Degrees of Freedom and Pseudospectral Discrete Hodge Operators, Unpublished, `http://www.cs.laurentian.ca/nrobidoux/prints/super/histogram.pdf`.

[15] E. Tonti, On the mathematical structure of a large class of physical theories. *Accademia Nazionale dei Lincei, estratto dai Rendiconti della Classe di Scienze fisiche, matematiche e naturali*, **Serie VIII**, **Vol. LII**, fasc. 1, Gennaio (1972).